nature ecology & evolution

ARTICLES

https://doi.org/10.1038/s41559-020-1281-8

A geometric basis for surface habitat complexity and biodiversity

Damaris Torres-Pulliza[1,2], Maria A. Dornelas[3], Oscar Pizarro[4], Michael Bewley[4], Shane A. Blowes[5,6], Nader Boutros[4], Viviana Brambilla[3], Tory J. Chase[7], Grace Frank[7], Ariell Friedman[4,8], Mia O. Hoogenboom[7], Stefan Williams[4], Kyle J. A. Zawada[3] and Joshua S. Madin[1]✉

Structurally complex habitats tend to contain more species and higher total abundances than simple habitats. This ecological paradigm is grounded in first principles: species richness scales with area, and surface area and niche density increase with three-dimensional complexity. Here we present a geometric basis for surface habitats that unifies ecosystems and spatial scales. The theory is framed by fundamental geometric constraints between three structure descriptors—surface height, rugosity and fractal dimension—and explains 98% of surface variation in a structurally complex test system: coral reefs. Then, we show how coral biodiversity metrics (species richness, total abundance and probability of interspecific encounter) vary over the theoretical structure descriptor plane, demonstrating the value of the theory for predicting the consequences of natural and human modifications of surface structure.

Most habitats on the planet are surface habitats—from the abyssal trenches to the tops of mountains, from coral reefs to the tundra. These habitats exhibit a broad range of structural complexities, from relatively simple, planar surfaces to highly complex three-dimensional (3D) structures. Currently, human and natural disturbances are changing the complexity of habitats faster than at any time in history[1–4]. Therefore, understanding and predicting the effects of habitat complexity changes on biodiversity is of paramount importance[5]. However, empirical relationships between commonly used descriptors of structural complexity and biodiversity are variable, often weak or contrary to expectation[6–10]. Moreover, there are no standards for quantifying structural complexity, precluding general patterns in the relationship between structure and diversity from being identified in different habitats. Therefore, we propose a new geometric basis for surface habitats that integrates and standardizes existing surface descriptors[8,10].

In theory, species richness scales with surface area according to a power law[11]. Island biogeography theory articulates that this relationship arises out of extinction and colonization since larger areas provide larger targets for species to colonize and a greater variety of habitats allowing species to coexist[12]. Our geometric theory builds on these ideas by exploring the notion that habitat surfaces with the same rugosity (defined as surface area per planar area in this study) can exhibit a range of different forms (Fig. 1). Total surface area is the integration of component areas at the smallest scale (that is, resolution), but it does not explain how these component areas fold and fill the 3D spaces they occupy. Rather, fractal dimension quantifies space filling at different scales[13]. Space filling promotes species coexistence by dividing surface area into a greater variety of structural elements[14], microhabitats and niches[15] (for example, high and low irradiance, small and large spaces, fast and slow flow). This variety of niches allows species to coexist (for example, different competitors or predator and prey[16]) and therefore enhances biodiversity[17,18]. We posit that there is a fundamental geometric constraint between surface rugosity and fractal dimension: for a given surface rugosity, an increase in fractal dimension will result in a reduction of the surface's mean height (Fig. 1). As the basis for a geometric theory, we mathematically derived the trade-off between

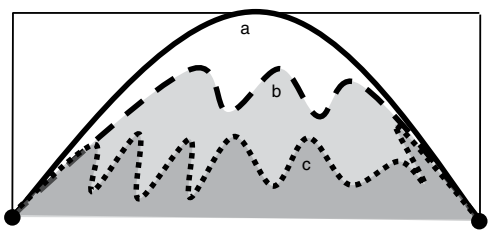

Fig. 1 | Increasing fractal dimension (that is, space filling) while keeping surface rugosity constant results in a decline in a surface's mean height range. Two-dimensional representation of three hypothetical surface habitats with the same surface rugosities, that is, the lengths of the lines in a–c are the same and occur over the same planar extent (black points). However, line 'a' fills less of its two-dimensional space (black rectangle) than does line 'c' and therefore has a lower fractal dimension.

[1]Hawai'i Institute of Marine Biology, University of Hawai'i at Mānoa, Kaneohe, HI, USA. [2]Department of Biological Sciences, Macquarie University, Sydney, New South Wales, Australia. [3]Centre for Biological Diversity, Scottish Oceans Institute, University of St Andrews, St Andrews, UK. [4]Australian Centre for Field Robotics, University of Sydney, Sydney, New South Wales, Australia. [5]German Centre for Integrative Biodiversity Research (iDiv) Halle-Jena-Leipzig, Leipzig, Germany. [6]Department of Computer Science, Martin Luther University Halle-Wittenberg, Halle, Germany. [7]ARC Centre of Excellence for Coral Reef Studies and College of Science and Engineering, James Cook University, Townsville, Queensland, Australia. [8]Greybits Engineering, Sydney, New South Wales, Australia. ✉e-mail: jmadin@hawaii.edu

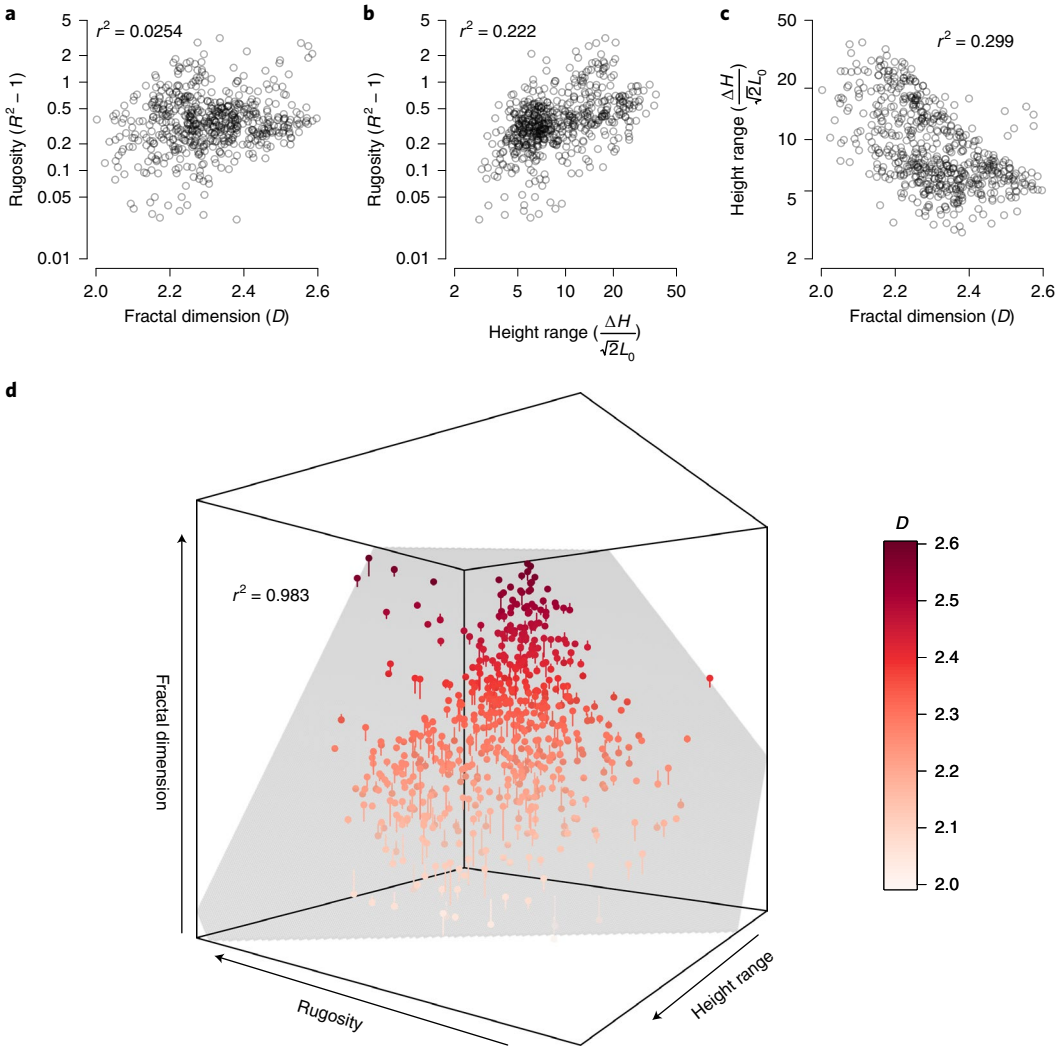

Fig. 2 | Comparison of the geometric theory with field data. a–c, Pairwise relationships between the descriptors that frame the geometric theory for $n = 595$ reef patches: surface rugosity (as $R^2 - 1$); fractal dimension (D); and surface height range (as $\frac{\Delta H}{\sqrt{2}L_0}$). Coefficients of determination (r^2) show the variance explained in the y-axis variable by the x-axis variable. **d**, When combined, the three descriptors explain more than 98% of the variation in fractal dimension D despite reef surfaces not being perfectly fractal (see Methods). Field data are represented by points and the surface descriptor plane is coloured by fractal dimension.

surface rugosity (R), fractal dimension (D) and surface height range (ΔH) as (see Methods for derivation):

$$\frac{1}{2}\log\left(R^2 - 1\right) + \log\left(\frac{L}{L_0}\right)(3 - D) = \log\left(\frac{\Delta H}{\sqrt{2}L_0}\right) \qquad (1)$$

where L is the surface linear extent and L_0 is the resolution (that is, the smallest scale of observation). R and D are both dimensionless, with $R \geq 1$ and $2 \leq D \leq 3$. ΔH is dimensionless when standardized by resolution L_0, with $\frac{\Delta H}{\sqrt{2}L_0} \geq 0$. When rugosity is expressed as $R^2 - 1$ (with $R^2 - 1 \geq 0$) and height range as $\frac{\Delta H}{\sqrt{2}L_0}$, equation (1) is a plane equation. Moreover, it is clear that any one of the surface descriptors can easily be expressed in terms of the other two, highlighting that any of the three variables is required but not sufficient alone to describe the structural complexity of a surface habitat.

Results

To test the theory, we examined associations between surface rugosity, fractal dimension and height range across coral reef habitat patches. Coral reefs are ideal ecosystems for testing a theory of surface habitats because they are structurally complex surface habitats constructed in large part by the reef-building scleractinian corals, which, in turn, live on the habitat (that is, corals are autogenic ecosystem engineers[19]). Structural complexity affects biodiversity in general[20] and of coral reefs in particular[21]. Using Structure from Motion, we estimated surface rugosity (expressed as the log of $R^2 - 1$), fractal dimension (D) and height range (as the log of $\frac{\Delta H}{\sqrt{2}L_0}$) from digital elevation models (DEMs) for 591 reef patches of 4 m^2 at 21 reef sites encircling Lizard Island on the Great Barrier Reef, Australia (see Methods). Analyses of the structure of these patches reveal that while rugosity, fractal dimension and surface height range are not independent, they have substantial independent variation (r^2 for pairwise relationships between surface descriptors ranging between 3% and 30%; Fig. 2a–c). However, when framed together, the three descriptors formed a plane, whereupon the trivially measured surface descriptors, rugosity and height range, captured 98% of the variation in D (Fig. 2d). The remaining 2% of the variation occurs because real surfaces do not necessarily behave like fractals (that is, are self-similar) across a wide range of scales (Extended Data Fig. 1). The observation that the structure of nearly all measured reef patches fell on a plane delineated by three simple surface descriptors highlights the fundamental geometric

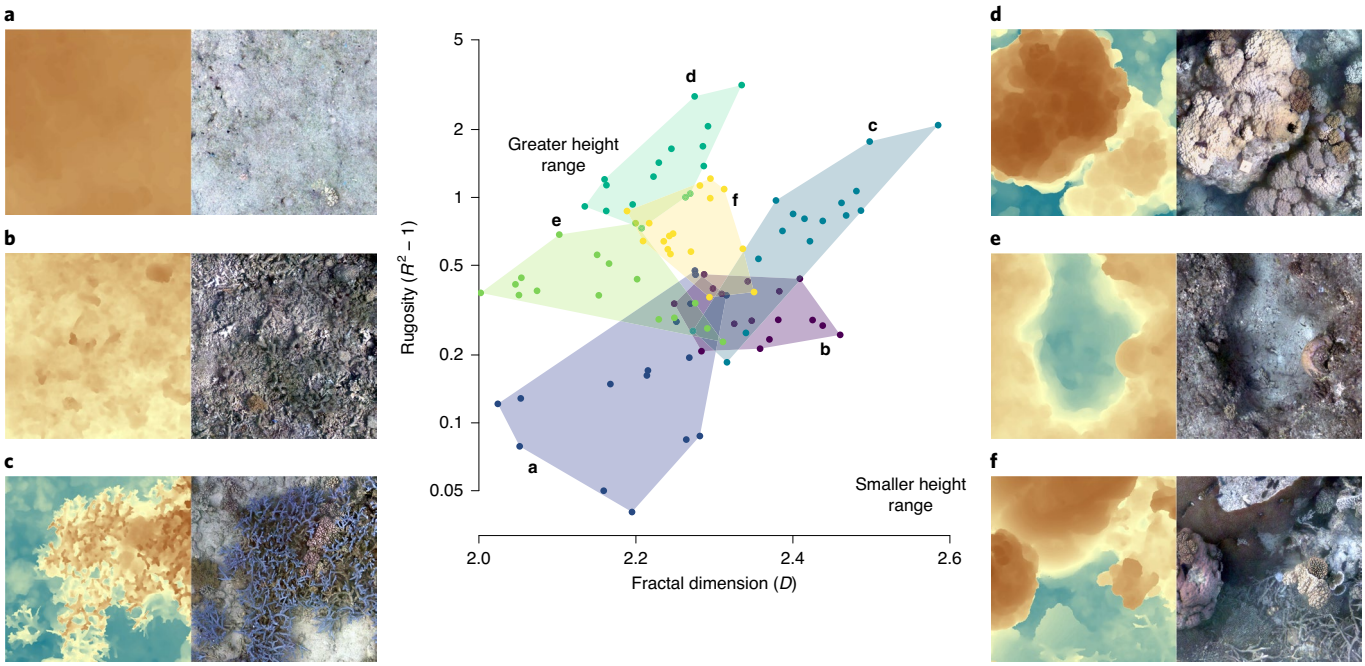

Fig. 3 | The geometric diversity of coral reef habitats. Reef patches ($n = 16$) from a subset of 6 sites are superimposed onto a two-dimensional representation of the surface descriptor plane (colour is used to delineate sites). **a**, North Reef. **b**, Osprey. **c**, Lagoon-2. **d**, Resort. **e**, South Island. **f**, Horseshoe (Extended Data Fig. 4). Patch height range is greater in the top left corner and decreases towards the bottom right corner. The corresponding DEMs and orthographic mosaics show selected patches at each site to help visualize geometric differences.

constraints of surface habitats. If fractal dimension increases, then either rugosity increases or height range decreases, or both. All three descriptors are essential for capturing structural complexity because they explain different elements of surface geometry: height range captures patch scale variation; rugosity captures fine scale variation, which sums to surface area; and fractal dimension captures the degree of space filling when transitioning from broad to fine scales (Extended Data Fig. 2a).

Different reef locations, with different ecological and environmental histories, occupied different regions on the surface descriptor plane (Fig. 3). For example, one site that was stripped of living coral during back-to-back tropical cyclones[22] largely occupied the region of the plane where rugosity, fractal dimension and surface height range are all low (Fig. 3a); that is, the patches at this site were closest to a theoretical flat surface. Another site also impacted by the cyclones but left littered with dead coral branches, had similar levels of rugosity and height range but fractal dimension was relatively high (Fig. 3b). In contrast, a site containing several large colonies of living branching coral had patches with the highest fractal dimension and rugosity, yet the height range of these patches was low (Fig. 3c) reflecting the approximately uniform height of living branching corals in shallow waters where water depth and tidal range constrains colony growth. Meanwhile, a site containing large hemispherical *Porites* corals had patches with large height ranges and high rugosity but lower fractal dimension (Fig. 3d). Three sites contained patches with similar distributions of rugosities (Fig. 3b,d,f) and therefore similar surface areas. However, these sites ranged from smooth reef surfaces with large holes (Fig. 3e) to highly bumpy surfaces with no holes (Fig. 3b), demonstrating why rugosity alone does not capture structural complexity and how varying mixtures of structural components dictate habitat complexity[14].

Finally, to connect the geometric variables to biodiversity, we examined how species richness, total abundance and diversity (measured as the probability of interspecific encounter[23]) varied across the surface descriptor plane. Strong ecological feedbacks occur between coral reef habitat structure and coral biodiversity metrics. Coral reef structures are largely created by corals, but their structure is mechanistically affected by environmental conditions such as tidal range, currents, storm impacts and wave exposure. For instance, coral larvae are poor swimmers and are more likely to settle in reef patches with small-scale complexity because they get entrapped by micro-eddies[24]. At the same time, more intricate coral structures (with higher fractal dimension, D) are more likely to be damaged or dislodged during storms that flatten reef patches[25,26]. Species–area theory predicts that species richness and abundances should be highest in patches with the greatest surface area[11] (that is, highest rugosity). We predicted that higher fractal dimension would also enhance species richness and abundance because of niche diversity (that is, increases in surface area at different scales), and that this effect would be additional to overall surface area. The surface descriptor plane allows estimating the combined effects of not just area but also niche differentiation associated with fractal dimension and height range[10,15].

We examined geometric-biodiversity coupling for a large plot, containing 261 of the 4-m^2 reef patches, where 9,264 coral colonies of 171 species were recorded (see Methods). Contrary to expectation, we found that all biodiversity metrics considered peaked in reef patches with intermediate surface rugosities. (Figure 4a shows diversity and Extended Data Fig. 7 includes species richness and abundance.) Indeed, several recent studies have argued that the relationship should be unimodal because, as complexity increases, the amount of area available for individuals to live declines[27,28]. However, biodiversity metrics also tended to increase monotonically in association with patches with higher fractal dimension and smaller height range (Extended Data Fig. 3). The explanatory power of reef geometry on biodiversity metrics was over 50% (Extended Data Fig. 8), which is 5–45% higher than any surface descriptor alone. Explaining this much variation in biodiversity is striking, given the number of other, non-geometric processes that govern coral biodiversity, including environmental filtering,

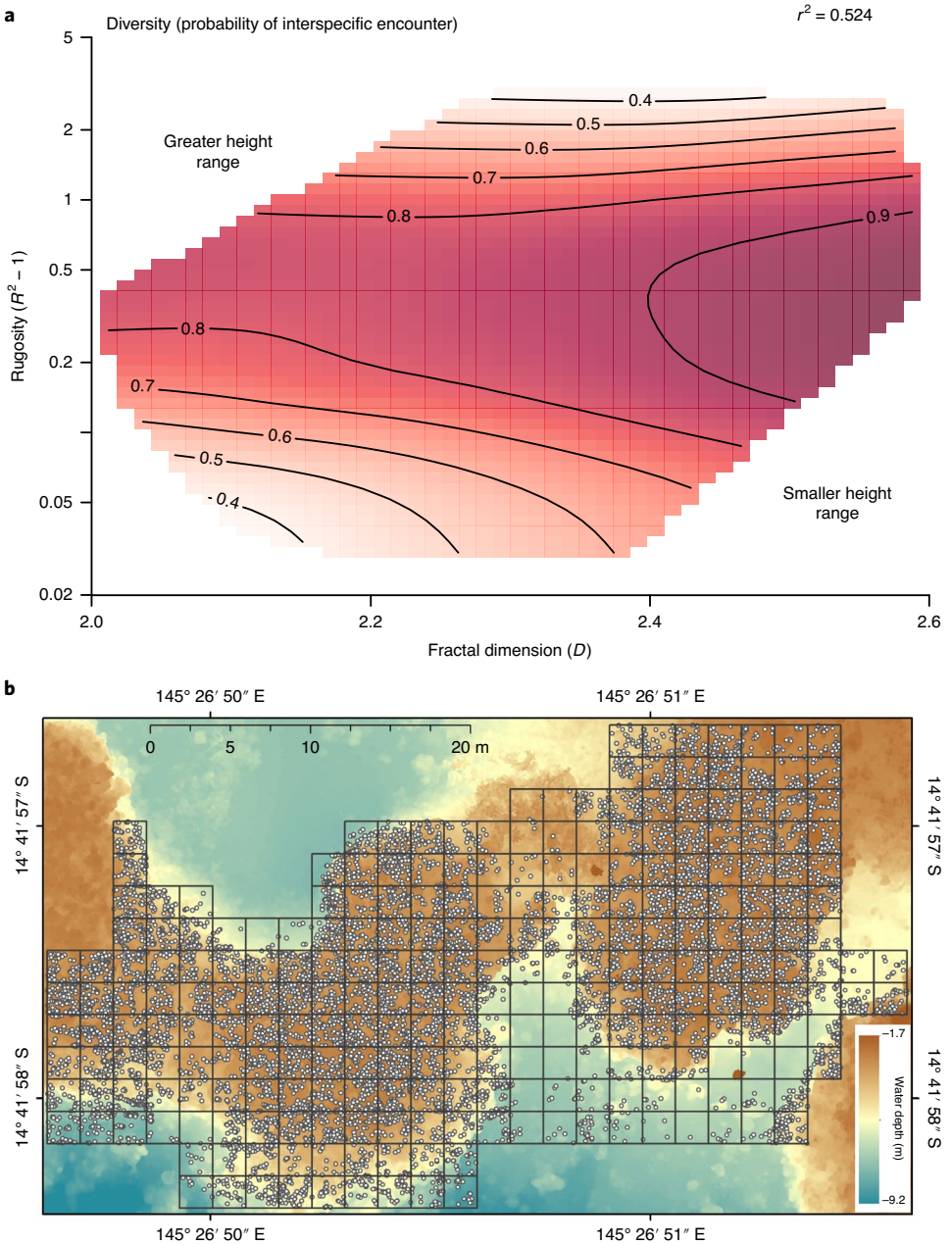

Fig. 4 | Geometric-biodiversity coupling of coral reef habitats. a, Predicted coral species diversity (represented as the probability of interspecific encounter) when plotted on the surface descriptor plane given by rugosity and fractal dimension. Height range is greater in the top left and decreases towards the bottom right as per equation (1). Prediction contours are from the general additive model summarized in Extended Data Fig. 7. **b**, DEM of the large plot with $n = 255$ contiguous 2 × 2 m reef patches (black squares) capturing 9,264 coral colony annotations (white points) representing 171 species.

dispersal and species interactions[29]. Because corals are autogenic ecosystem engineers, reciprocal causality is likely to strengthen and shape geometric-biodiversity coupling. For instance, high rugosity is often generated by large hemispherical corals (for example, see Fig. 3d) that reduce the number of individuals and hence species per area[14]. Subsequently, geometric-biodiversity coupling may be weaker for other surface-associated taxa, such as fishes and invertebrates, and should be tested. Nonetheless, our findings have implications for resilience following disturbances and for restoration efforts that aim to maximize biodiversity[30], specifically identifying the reef structural characteristics that should be maintained (or built) to maximize biodiversity.

Discussion

A general, scale-independent geometric basis for surface habitats provides a much needed way to quantify habitat complexity across ecosystems and spatial scales. Meanwhile, creating 3D habitat surfaces is becoming increasingly accessible and cost-effective, for example, using Structure from Motion[31,32], both underwater and on land. The importance of surface complexity as a determinant of habitat condition, biodiversity and ecosystem function is well recognized[33], yet different metrics are typically used for different ecosystems, or different taxa within the same ecosystem[10]. The general quantitative approach we propose is applicable across surface habitats in both marine and terrestrial environments, allowing formal

comparisons examining whether geometric-biodiversity couplings differ between systems in terms of both pattern and strength. The surface descriptor plane uncovered in this study clearly defines the fundamental geometric constraints acting to shape surface habitats, and consequently how changes in surface geometry affect biodiversity. Nonetheless, there are several unknowns about the surface descriptor plane and its associations with biodiversity metrics that require further exploration. These unknowns range from technical limitations (for example, how does the theory translate from DEMs that exclude overhanging surfaces to 3D surface meshes?) to ecological patterns (for example, how do different types of structural components, such as different mixtures of branching and hemispherical corals or live and dead elements[14,34], mediate geometric-biodiversity coupling?).

As powerful ecosystem engineers, humans are modifying the planet through the structures we destroy, both physically and indirectly via environmental change[4], and those we construct. Indeed, human-modified structures differ significantly in their geometry from nature-built structures[35]. Determining how biodiversity, conservation status and recovery rates relate to habitat complexity measures is paramount in the Anthropocene. The approach we propose in this study allows for predictions of the biodiversity consequences of these structural changes across land and seascapes.

Methods

Geometric theory for surface habitats. The variation method for calculating fractal dimension D measures the mean height range of a surface at different scales[36,37]. At the broadest scale, the linear extent L, the surface height range is ΔH (Extended Data Fig. 2a). At the finest scale, the resolution L_0, the height range (ΔH_0) is the mean of height ranges of all the component areas at that scale. The slope S of the resulting log-log relationship (shown in Extended Data Fig. 2a) is:

$$S = \frac{\log(\Delta H) - \log(\Delta H_0)}{\log(L) - \log(L_0)} \tag{2}$$

where fractal dimension is[37]:

$$D = 3 - S \tag{3}$$

Rearranging equation (2) gives:

$$S = \frac{\log(\Delta H/\Delta H_0)}{\log(L/L_0)} \tag{4}$$

Surface area A can be estimated by summing areas A_0 at the finest grain L_0. Given the mean height range ΔH_0 at L_0, we assume that any finer-scale detail is not observable and we calculate A_0 from the minimal surface consistent with ΔH_0 (Extended Data Fig. 2b) as:

$$A_0 = \frac{L_0}{2}\sqrt{2\Delta H_0{}^2 + 4L_0^2} \tag{5}$$

and then multiply by the number of component areas $\left(\frac{L^2}{L_0^2}\right)$ giving:

$$A = \frac{L^2}{2L_0}\sqrt{2\Delta H_0{}^2 + 4L_0^2} \tag{6}$$

Surface rugosity is[32]:

$$R = \frac{A}{L^2} \tag{7}$$

Substituting A for equation (6) and rearranging gives:

$$R = \sqrt{\frac{\Delta H_0{}^2}{2L_0^2} + 1} \tag{8}$$

Rearranging for ΔH_0 gives:

$$\Delta H_0 = \sqrt{2}L_0\sqrt{R^2 - 1} \tag{9}$$

and substituting into equation (4) gives:

$$S = \frac{\log\left(\frac{\Delta H}{\sqrt{2}L_0\sqrt{R^2-1}}\right)}{\log\left(\frac{L}{L_0}\right)} \tag{10}$$

This leads to:

$$D = 3 - \frac{\log\left(\frac{\Delta H}{\sqrt{2}L_0\sqrt{R^2-1}}\right)}{\log\left(\frac{L}{L_0}\right)} \tag{11}$$

Further rearranging gives a plane as equation (1) in the main text. The boundary equations for the limits of fractal dimension D are:

$$\Delta H_{D=2} = \sqrt{2}L\sqrt{R^2 - 1} \tag{12}$$

$$\Delta H_{D=3} = \sqrt{2}L_0\sqrt{R^2 - 1} \tag{13}$$

Coral reef surface field study. Twenty-one reef flat sites were selected approximately 1 km apart and encircling Lizard Island on the Great Barrier Reef, Australia (Extended Data Fig. 4). The spatial arrangement of the sites captured a broad range of habitats that were shaped predominantly by wave exposure generated by prevailing south-east trade winds[22]. Mean water depth across all study sites ranges between 2 and 3.5 m. In 2014, at the trimodal site, we used an Iver2 Autonomous Underwater Vehicle[38] to collect 45,000 georeferenced overlapping, stereo-pair images of an approximately 30 × 50 m section of the reef crest (Fig. 4b). In 2016, at all 21 sites, we used the spiral method[39], which involves swimming a camera rig that unspools from a central point to capture approximately 3,000 overlapping, stereo-pair images of approximately 130 m^2 of reef crest (Extended Data Fig. 5). We used a simultaneous localization and mapping approach[40] fusing global positioning system, stereo imagery and altitude information to provide an initial pose estimate for the cameras. We used the Agisoft Metashape software (version 1.6.3) to process the images and produce a 3D dense cloud from which we derived a gridded DEM and orthographic mosaic for coral annotation per site. The output resolution of all DEMs was 0.002 m. We used DEMs to exclude overhanging surfaces (that is, only one height for each xy combination) because the degree to which overhangs are captured from plan view photographic surveys is biased by the changing lighting conditions of the environment[41] (for example, the sun angle, cloud cover, water turbidity). On the other hand, plan view surveys were preferred to reduce the time costs associated with capturing stereo pairs from multiple view angles over large areas. The use of DEMs underestimates surface rugosity and fractal dimension, that is, the reason why D tended to range below 2.6. However, given that overhanging structures were rare at our study sites, R and D measures are likely to exhibit the correct rank order for patches.

Given the lack of coral cover following the 2016 mass bleaching event on the Great Barrier Reef[22], we used the 2014 trimodal large plot to quantify geometric biodiversity relationships (Extended Data Fig. 4, red box). The plot was divided into a contiguous grid of 2 × 2 m reef patches (Fig. 4b, black squares). Patches of the orthographic mosaic were printed on underwater paper and used as reference maps for in situ identification of all coral colonies of diameter >5 cm to species by a team of 6 researchers over 4 weeks. We focused on the reef crest and flat (shallower areas in Fig. 4b) but also included the reef edge and deeper reef. Colonies of unknown or hard to identify species were photographed and identified in consultation with guidebooks and other observers. Hemispherical *Porites* colonies were identified to the genus level due to the difficulty differentiating between the few known species without collecting samples for microscopy. Colony annotations were digitized over the orthographic mosaic using the QGIS software (version 3.4) (for example, Fig. 4b, white points). Only scleractinian corals were included for analysis. In total, 9,264 coral colonies of 171 species were observed within the 255 reef patches censused. Diversity was calculated as the probability of interspecific encounter or 1 − Simpson diversity[23].

Each of the circular DEMs had a central point from which an 8 by 8 m square was centred (Extended Data Fig. 5) and divided into 16 contiguous reef patches of 2 × 2 m. DEMs for each 2 × 2 m patch from both the trimodal large plot (where corals were censused) and the 21 circular plots were cropped to calculate surface rugosity R, fractal dimension D and the height range of the patch ΔH, the latter being the difference between the deepest and shallowest point in a patch. D was calculated using the variation method[37]; each patch was divided into squares with sides lengths (L) of 2, 1, 0.5, 0.25, 0.125, 0.0625 and 0.03125 m capturing approximately 2 orders of magnitude[42]. The resolution L_0 for the theory is the smallest scale (that is, 0.03125 m). The height ranges within each grid at each scale were calculated and then averaged for that scale to avoid weighting the many estimates at smaller scales more than the fewer estimates at larger scales when calculating the slope S. S was calculated for each patch by fitting a linear model to the log of scale (that is, grid sizes) versus the log of mean height. D was then calculated according to equation (3). R was calculated according to equation (8). There are many ways to estimate the surface area of a DEM, so we compared surface rugosity calculated from theory (equation (8)) with estimates based on surface area calculations using the surfaceArea function in the package sp[43] (version 1.3.2). The theory underestimated surface rugosity by approximately 5% (Extended Data Fig. 6) because of the minimal area assumption (Extended Data Fig. 2b), but this disparity was consistent across the range of rugosities.

Analyses. Surface rugosity (expressed as $R^2 - 1$) and standardized height range (expressed as $\frac{\Delta H}{\sqrt{2L_0}}$) were base-10 log-transformed as per the plane equation (equation (1)). Species richness and abundance were square root-transformed and diversity was arcsin-transformed for all analyses to improve model residuals. Coefficients of determination (r^2) of pairwise associations of the three geometric variables were estimated by squaring Pearson correlation coefficients. Reef surfaces were not perfectly fractal: mean height ranges at L and L_0 anchor the theory (Extended Data Fig. 2a) but mean height ranges at scales intermediate to L and L_0 could shift the overall relationship, albeit subtly. Therefore, we calculated the r^2 for the surface descriptor plane based on the deviances of empirically derived D from theory-derived D (Extended Data Fig. 1), that is, by dividing the residual sums of squares by the total sums of squares and then subtracting this value from 1.

We quantified geometric-biodiversity relationships for the large plot at the trimodal site using both generalized additive models (GAMs) and linear models. We applied the default smoother term to each surface descriptor for the GAMs and second-order polynomials for the linear models to allow for nonlinear relationships between predictor and response variables. We quantified the effect of each geometric variable separately on species richness, total abundance and diversity (probability of interspecific encounter) and then all together to assess improvement in explained variation as adjusted r^2 values (Extended Data Figs. 3 and 8). We included the three reef patches with no living coral but also confirmed that removing these points had no discernible influence on the geometric-biodiversity relationships. We also ran analyses after the removal of the 5–6 highest rugosity patches that appeared to be largely responsible for producing the hump-shaped rugosity-biodiversity relationships (Extended Data Fig. 3, red curves). Smooth terms for rugosity and height range were significant, with reference d.f. much greater than one for all biodiversity metrics, suggesting significant nonlinear effects for these surface descriptors[44]. Fractal dimension showed a linear effect for richness and diversity; thus, the smoother term was removed for these analyses. Residuals for all models were approximately normal and were homogeneous when plotted against predictor variables. The linear models with second-order polynomial terms gave the same overall results as GAMs (Extended Data Fig. 3), that is, the polynomial term was significant for the same terms that retained the smoother function in the GAMs. However, the linear models had lower adjusted r^2 values and so we presented the final results using the GAMs (Fig. 4a and Extended Data Fig. 7).

All analyses, including model selection and diagnostics and figure creation, were conducted in R[45] (version 3.6.1) and can be downloaded or cloned at GitHub (https://github.com/jmadin/surface_geometry).

Reporting Summary. Further information on research design is available in the Nature Research Reporting Summary linked to this article.

Data availability

Source data for statistical analyses and figures are available at https://github.com/jmadinlab/surface_geometry.

Code availability

Code for data preparation, statistical analyses and figures is available at https://github.com/jmadinlab/surface_geometry.

Received: 6 February 2020; Accepted: 17 July 2020;
Published online: 24 August 2020

References

1. Pimm, S. L. et al. The biodiversity of species and their rates of extinction, distribution, and protection. *Science* **344**, 1246752 (2014).
2. Newbold, T. et al. Global effects of land use on local terrestrial biodiversity. *Nature* **520**, 45–50 (2015).
3. Alvarez-Filip, L., Dulvy, N. K., Gill, J. A., Côté, I. M. & Watkinson, A. R. Flattening of Caribbean coral reefs: region-wide declines in architectural complexity. *Proc. Biol. Sci.* **276**, 3019–3025 (2009).
4. Millennium Ecosystem Assessment *Ecosystems and Human Well-Being: Synthesis* (Island Press, 2005).
5. Schulze, E. D. & Mooney, H. A. *Biodiversity and Ecosystem Function* (Springer, 1993).
6. Pimm, S. L. The complexity and stability of ecosystems. *Nature* **307**, 321–326 (1984).
7. Morse, D. R., Lawton, J. H., Dodson, M. M. & Williamson, M. H. Fractal dimension of vegetation and the distribution of arthropod body lengths. *Nature* **314**, 731–733 (1985).
8. McCoy, E. D. & Bell, S. S. in *Habitat Structure: the Physical Arrangement of Objects in Space* (eds Bell, S. S. et al.) 3–27 (Springer, 1991).
9. Beck, M. W. Separating the elements of habitat structure: independent effects of habitat complexity and structural components on rocky intertidal gastropods. *J. Exp. Mar. Biol. Ecol.* **249**, 29–49 (2000).
10. Kovalenko, K. E., Thomaz, S. M. & Warfe, D. M. Habitat complexity: approaches and future directions. *Hydrobiologia* **685**, 1–17 (2012).
11. Arrhenius, O. Species and area. *J. Ecol.* **9**, 95–99 (1921).
12. MacArthur, R. H. & Wilson, E. O. *The Theory of Island Biogeography* (Princeton Univ. Press, 1967).
13. Mandelbrot, B. B. *The Fractal Geometry of Nature* (W. H. Freeman, 1983).
14. Tokeshi, M. & Arakaki, S. Habitat complexity in aquatic systems: fractals and beyond. *Hydrobiologia* **685**, 27–47 (2012).
15. Johnson, M. P., Frost, N. J., Mosley, M. W. J., Roberts, M. F. & Hawkins, S. J. The area-independent effects of habitat complexity on biodiversity vary between regions. *Ecol. Lett.* **6**, 126–132 (2003).
16. Chesson, P. Mechanisms of maintenance of species diversity. *Annu. Rev. Ecol. Syst.* **31**, 343–366 (2000).
17. Pianka, E. R. *Evolutionary Ecology* (Harper and Row, 1988).
18. Sugihara, G. & May, R. M. Applications of fractals in ecology. *Trends Ecol. Evol.* **5**, 79–86 (1990).
19. Jones, C. G., Lawton, J. H. & Shachak, M. Positive and negative effects of organisms as physical ecosystem engineers. *Ecology* **78**, 1946–1957 (1997).
20. Brown, J. H. et al. The fractal nature of nature: power laws, ecological complexity and biodiversity. *Phil. Trans. R. Soc. B* **357**, 619–626 (2002).
21. Graham, N. A. J. & Nash, K. L. The importance of structural complexity in coral reef ecosystems. *Coral Reefs* **32**, 315–326 (2013).
22. Madin, J. S. et al. Cumulative effects of cyclones and bleaching on coral cover and species richness at Lizard Island. *Mar. Ecol. Prog. Ser.* **604**, 263–268 (2018).
23. Hurlbert, S. H. The nonconcept of species diversity: a critique and alternative parameters. *Ecology* **52**, 577–586 (1971).
24. Hata, T. et al. Coral larvae are poor swimmers and require fine-scale reef structure to settle. *Sci. Rep.* **7**, 2249 (2017).
25. Madin, J. S. & Connolly, S. R. Ecological consequences of major hydrodynamic disturbances on coral reefs. *Nature* **444**, 477–480 (2006).
26. Alvarez-Filip, L. et al. Drivers of region-wide declines in architectural complexity on Caribbean reefs. *Coral Reefs* **30**, 1051–1060 (2011).
27. Allouche, O., Kalyuzhny, M., Moreno-Rueda, G., Pizarro, M. & Kadmon, R. Area-heterogeneity tradeoff and the diversity of ecological communities. *Proc. Natl Acad. Sci. USA* **109**, 17495–17500 (2012).
28. Paxton, A. B., Pickering, E. A., Adler, A. M., Taylor, J. C. & Peterson, C. H. Flat and complex temperate reefs provide similar support for fish: evidence for a unimodal species-habitat relationship. *PLoS ONE* **12**, e0183906 (2017).
29. Huston, M. A. Patterns of species diversity on coral reefs. *Annu. Rev. Ecol. Syst.* **16**, 149–177 (1985).
30. Loke, L. H. L., Todd, P. A., Ladle, R. J. & Bouma, T. J. Creating complex habitats for restoration and reconciliation. *Ecol. Eng.* **77**, 307–313 (2015).
31. Young, G. C., Dey, S., Rogers, A. D. & Exton, D. Cost and time-effective method for multi-scale measures of rugosity, fractal dimension, and vector dispersion from coral reef 3D models. *PLoS ONE* **12**, e0175341 (2017).
32. Friedman, A., Pizarro, O., Williams, S. B. & Johnson-Roberson, M. Multi-scale measures of rugosity, slope and aspect from benthic stereo image reconstructions. *PLoS ONE* **7**, e50440 (2012).
33. Weiher, E. & Keddy, P. A. *Ecological Assembly Rules: Perspectives, Advances, Retreats* (Cambridge Univ. Press, 2001).
34. Bartholomew, A., Diaz, R. J. & Cicchetti, G. New dimensionless indices of structural habitat complexity: predicted and actual effects on a predator's foraging success. *Mar. Ecol. Prog. Ser.* **206**, 45–58 (2000).
35. Strain, E. M. A. et al. Eco-engineering urban infrastructure for marine and coastal biodiversity: which interventions have the greatest ecological benefit? *J. Appl. Ecol.* **55**, 426–441 (2018).
36. Dubuc, B., Zucker, S. W., Tricot, C., Quiniou, J. F. & Wehbi, D. Evaluating the fractal dimension of surfaces. *Proc. R. Soc. Lond. A Math. Phys. Sci.* **425**, 113–127 (1989).
37. Zhou, G. & Lam, N. S.-N. A comparison of fractal dimension estimators based on multiple surface generation algorithms. *Comput. Geosci.* **31**, 1260–1269 (2005).
38. Johnson-Roberson, M. et al. High-resolution underwater robotic vision-based mapping and three-dimensional reconstruction for archaeology. *J. Field Robot.* **34**, 625–643 (2017).
39. Pizarro, O., Friedman, A., Bryson, M., Williams, S. B. & Madin, J. A simple, fast, and repeatable survey method for underwater visual 3D benthic mapping and monitoring. *Ecol. Evol.* **7**, 1770–1782 (2017).
40. Mahon, I., Williams, S. B., Pizarro, O. & Johnson-Roberson, M. Efficient view-based SLAM using visual loop closures. *IEEE Trans. Robot.* **24**, 1002–1014 (2008).
41. Bryson, M. et al. Characterization of measurement errors using structure-from-motion and photogrammetry to measure marine habitat structural complexity. *Ecol. Evol.* **7**, 5669–5681 (2017).
42. Zawada, D. G. & Brock, J. C. A multi-scale analysis of coral reef topographic complexity using Lidar-derived bathymetry. *J. Coast. Res.* **10053**, 6–15 (2009).
43. Bivand, R. S., Pebesma, E. & Gómez-Rubio, V. *Applied Spatial Data Analysis with R* (Springer, 2013).
44. Wood, S. N., Pya, N. & Säfken, B. Smoothing parameter and model selection for general smooth models. *J. Am. Stat. Assoc.* **111**, 1548–1563 (2016).

45. R Core Team *R: A Language and Environment For Statistical Computing* (R Foundation for Statistical Computing, 2019).

Acknowledgements
We thank A. Hoggett and L. Vail of the Lizard Island Research Station for their support. This work was supported by an Australian Research Council Future Fellowship (to J.S.M.), the John Templeton Foundation (to M.A.D. and J.S.M.), a Royal Society research grant and a Leverhulme Fellowship (to M.A.D.), an International Macquarie University Research Excellence Scholarship (to D.T.-P.), two Ian Potter Doctoral Fellowships at Lizard Island (to D.T.-P. and V.B.) and an Australian Endeavour Scholarship (to T.J.C.).

Author contributions
J.S.M., D.T.-P., M.A.D. and O.P. conceptualized the study. J.S.M. and O.P. developed the theory and J.S.M. ran the analyses. J.S.M., D.T.-P. and O.P. developed the software pipeline for the data and produced the visualizations. J.S.M., D.T.-P., M.A.D. and O.P. led the investigation. J.S.M. and M.A.D. led and funded the broader project, with additional field robotics resources provided by O.P. and S.W. D.T.-P., M.A.D., O.P., M.B., S.A.B., N.B., V.B., T.J.C., G.F., A.F., M.O.H., S.W., K.J.A.Z. and J.S.M. collected the data. J.S.M. wrote the first draft of the paper and all authors reviewed at least one draft.

Competing interests
The authors declare no competing interests.

Additional information
Extended data is available for this paper at https://doi.org/10.1038/s41559-020-1281-8.

Supplementary information is available for this paper at https://doi.org/10.1038/s41559-020-1281-8.

Correspondence and requests for materials should be addressed to J.S.M.

Reprints and permissions information is available at www.nature.com/reprints.

Publisher's note Springer Nature remains neutral with regard to jurisdictional claims in published maps and institutional affiliations.

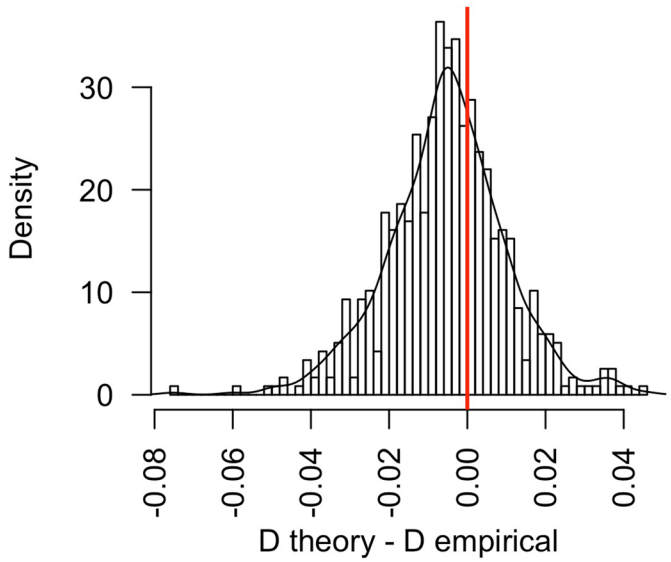

Extended Data Fig. 1 | Differences in fractal dimension when calculated empirically versus from the theory that assumes self-similarity across scales.

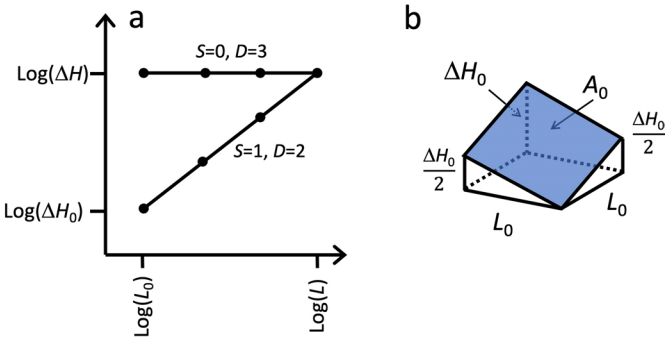

Extended Data Fig. 2 | Geometric theory for surface habitats. a, Schematic showing mean height variation as a function of scale. ΔH is the height range of the habitat surface for the extent L. ΔH_0 is the mean height range of the surface at the smallest scale: the resolution L_0. The two slopes S represent fractal dimensions D of 2 and 3 according to Eq. 2. For example, high D results when mean height ranges at the scale of the grain are large (that is, in the vicinity of ΔH), suggesting a highly convoluted surface. Conversely, low D occurs when mean height variations at the scale of the grain are very small, suggesting an approximately flat surface. **b**, Area A_0 at the scale of the grain L_0 is calculated as the minimum surface area given the mean height range at this scale.

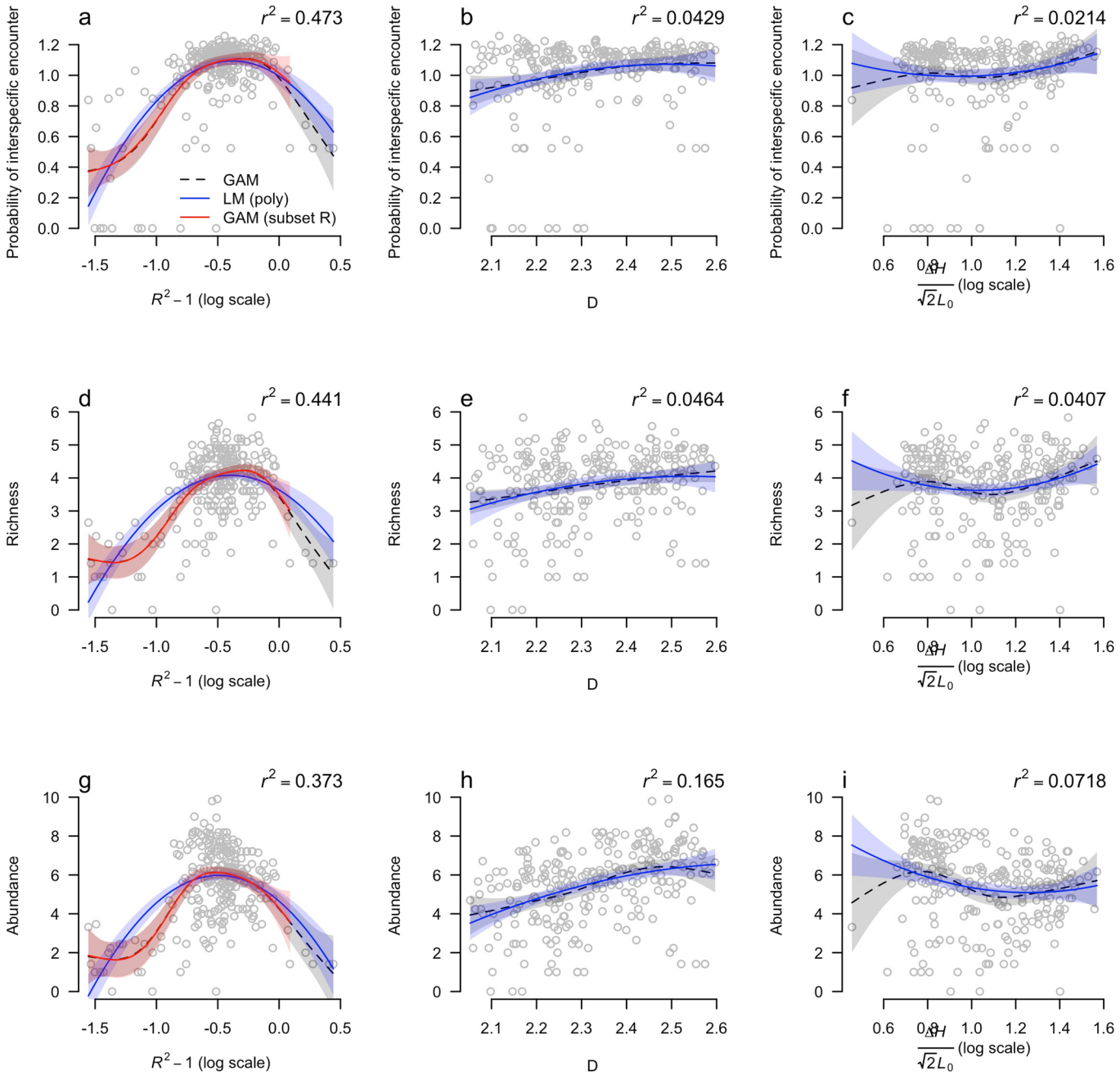

Extended Data Fig. 3 | Underlying empirical data and models fits (±95% confidence intervals) for all combinations of the three surface descriptors (x-axes) and species richness, abundance and diversity (PIE) (y-axes). The overall pattern was captured by both statistical approaches: generalised additive models and linear models with second-order polynomials for each surface descriptors. r^2 values were consistently better for GAMs and reported here and in Extended Data Fig. 8.

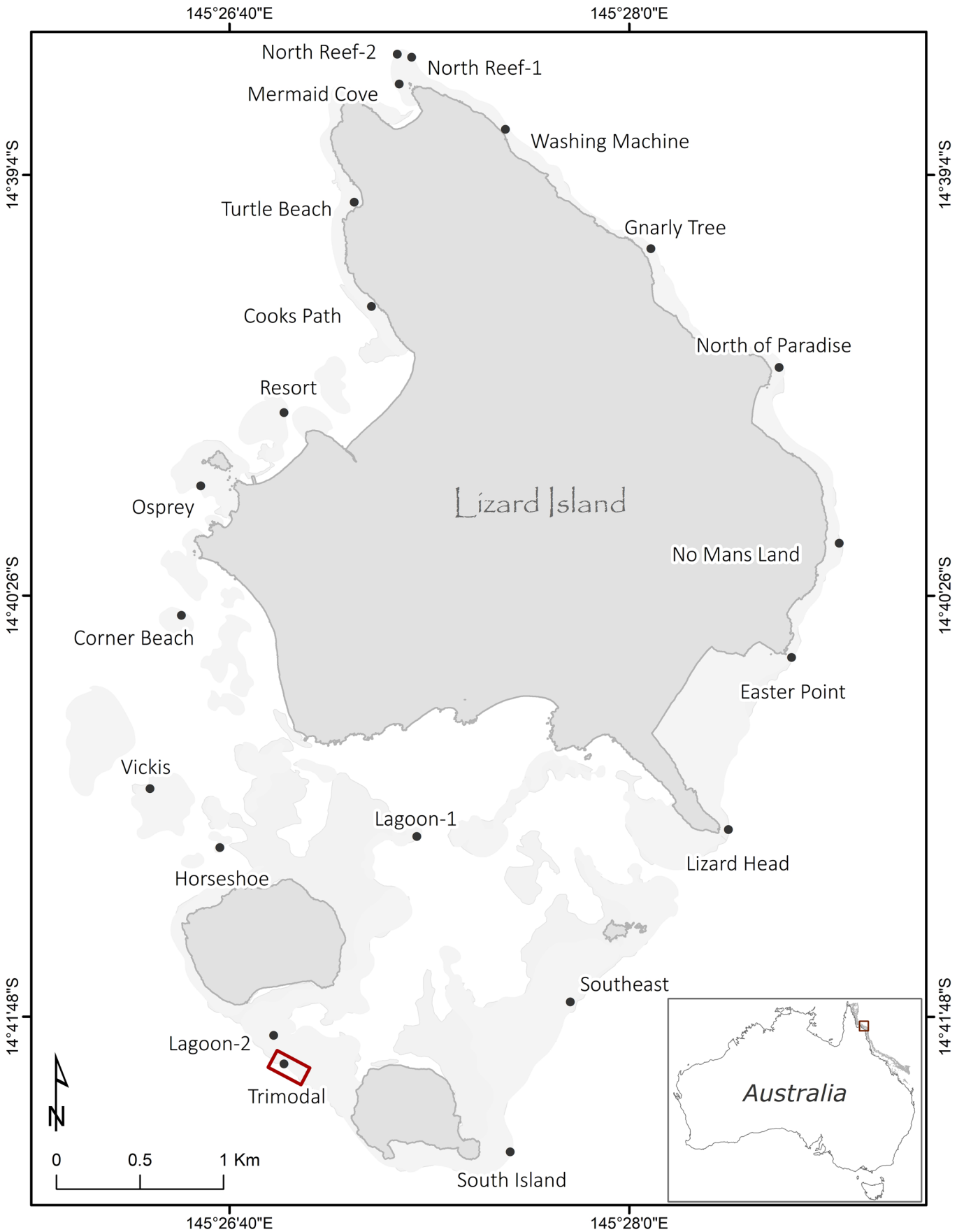

Extended Data Fig. 4 | The 21 shallow reef flat locations (black points) and the large Trimodal plot (red box) at Lizard Island, the Great Barrier Reef, Australia.

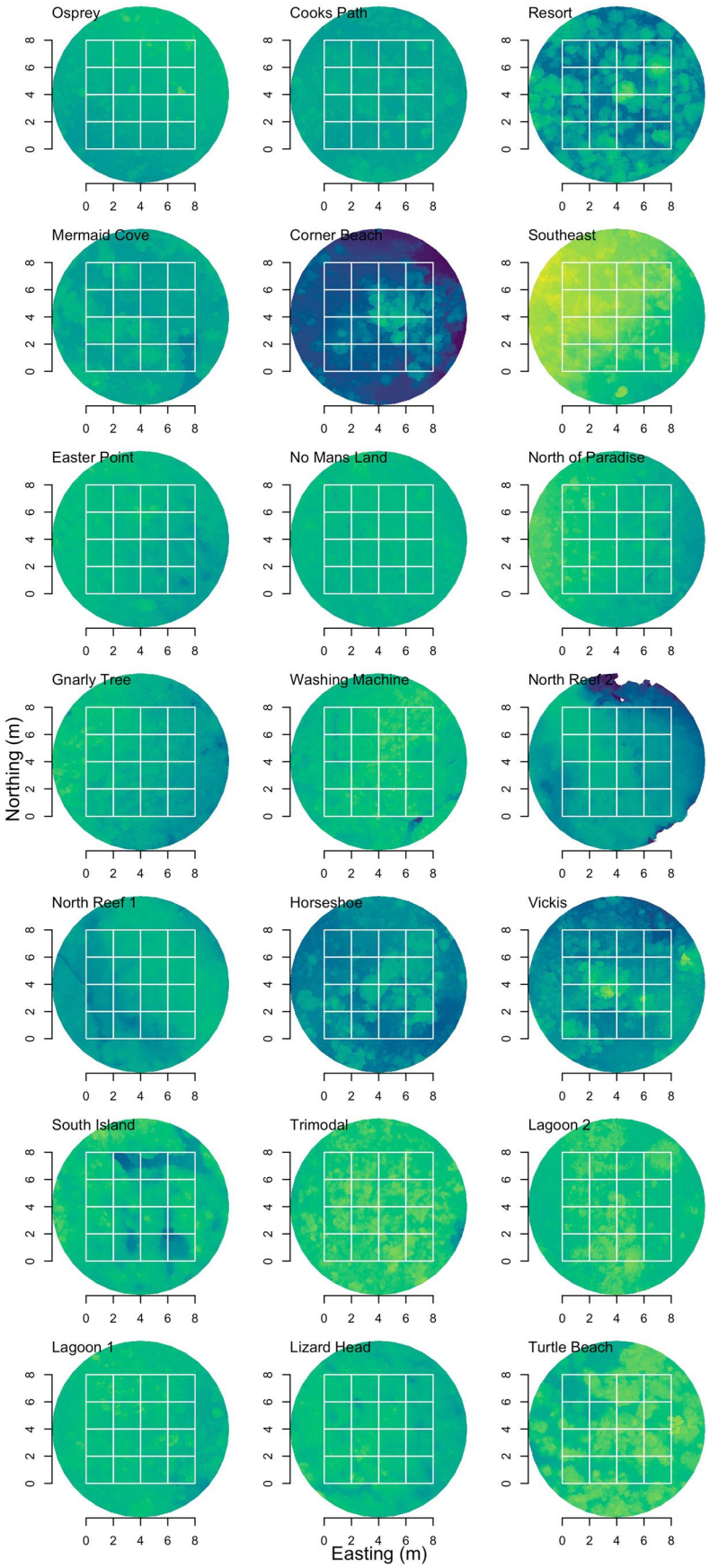

Extended Data Fig. 5 | Digital elevation models of the 21 reef sites capturing different habitats encircling Lizard Island (see Extended Data Fig. 4 for map). The models show the 2 m by 2 m reef patches (white squares) and depth gradience from 1.5m (lightest green) to 5m depth (darkest blue).

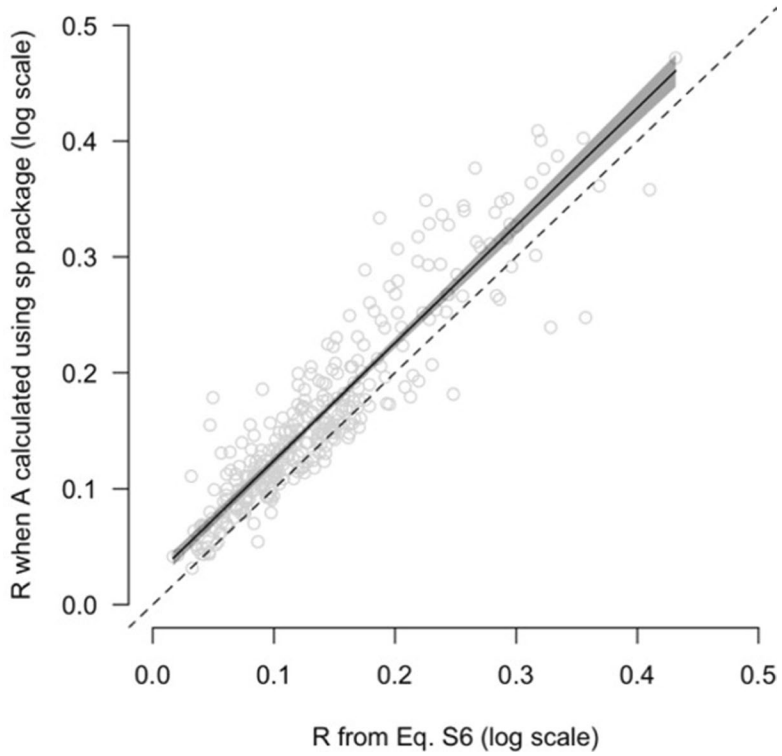

Extended Data Fig. 6 | The relationship between R when calculated from the geometric theory for habitat surfaces and when calculated using surface area calculated using a spatial statistics function. Dashed line is the unity line. Black line is the fit of a linear model (intercept: 0.023 ± 0.007 95% confidence intervals; slope: 1.014 ± 0.046 95% confidence intervals which encapsulates 1).

Model	**a** Richness r^2	**b** Abundance r^2	**c** Diversity r^2
$\log_{10}(R^2\text{-}1)$	0.441	0.373	0.473
D	0.046	0.165	0.043
$\log_{10}(\frac{\Delta H}{\sqrt{2}L_0})$	0.041	0.072	0.021
$\log_{10}(R^2\text{-}1) + D + \log_{10}(\frac{\Delta H}{\sqrt{2}L_0})$	0.514	0.514	0.524

Extended Data Fig. 7 | Model parameter and smooth term estimates for the best-fit species richness (a), abundance (b) and diversity (PIE) GAMs (c). N =255.

a Species richness				
Parametric terms	*Estimate*	*Std. Error*	*t value*	*Pr(>|t|)*
D	1.624	0.021	77.23	<< 0.001
Smooth terms	*edf*	*Ref.df*	*F*	*p-value*
$\log_{10}(R^2\text{-}1)$	5.496	6.651	28.016	<< 0.001
$\log_{10}(\frac{\Delta H}{\sqrt{2}L_0})$	3.204	4.069	3.842	0.004

b Abundance				
Parametric terms	*Estimate*	*Std. Error*	*t value*	*Pr(>|t|)*
D	2.346	0.037	62.92	<< 0.001
Smooth terms	*edf*	*Ref.df*	*F*	*p-value*
$\log_{10}(R^2\text{-}1)$	5.695	6.860	26.875	<< 0.001
$\log_{10}(\frac{\Delta H}{\sqrt{2}L_0})$	3.139	3.989	6.876	<< 0.001

c Diversity				
Parametric terms	*Estimate*	*Std. Error*	*t value*	*Pr(>|t|)*
D	0.438	0.005	92.28	<< 0.001
Smooth terms	*edf*	*Ref.df*	*F*	*p-value*
$\log_{10}(R^2\text{-}1)$	5.145	6.273	29.840	<< 0.001
$\log_{10}(\frac{\Delta H}{\sqrt{2}L_0})$	2.988	3.799	3.646	0.007

Extended Data Fig. 8 | Adjusted r^2 values for GAM models of species richness (a), total abundance (b) and diversity (PIE) (c) with each of the three geometric variables and the best combined model after model selection. $N = 255$.

nature research

Corresponding author(s): Joshua S Madin

Last updated by author(s): Jul 9, 2020

Reporting Summary

Nature Research wishes to improve the reproducibility of the work that we publish. This form provides structure for consistency and transparency in reporting. For further information on Nature Research policies, see Authors & Referees and the Editorial Policy Checklist.

Statistics

For all statistical analyses, confirm that the following items are present in the figure legend, table legend, main text, or Methods section.

n/a	Confirmed	
☐	☒	The exact sample size (*n*) for each experimental group/condition, given as a discrete number and unit of measurement
☐	☒	A statement on whether measurements were taken from distinct samples or whether the same sample was measured repeatedly
☐	☒	The statistical test(s) used AND whether they are one- or two-sided *Only common tests should be described solely by name; describe more complex techniques in the Methods section.*
☐	☒	A description of all covariates tested
☐	☒	A description of any assumptions or corrections, such as tests of normality and adjustment for multiple comparisons
☐	☒	A full description of the statistical parameters including central tendency (e.g. means) or other basic estimates (e.g. regression coefficient) AND variation (e.g. standard deviation) or associated estimates of uncertainty (e.g. confidence intervals)
☐	☒	For null hypothesis testing, the test statistic (e.g. *F*, *t*, *r*) with confidence intervals, effect sizes, degrees of freedom and *P* value noted *Give P values as exact values whenever suitable.*
☒	☐	For Bayesian analysis, information on the choice of priors and Markov chain Monte Carlo settings
☒	☐	For hierarchical and complex designs, identification of the appropriate level for tests and full reporting of outcomes
☐	☒	Estimates of effect sizes (e.g. Cohen's *d*, Pearson's *r*), indicating how they were calculated

Our web collection on statistics for biologists contains articles on many of the points above.

Software and code

Policy information about availability of computer code

Data collection	Data were extracted from images collected in the field using Agisoft Metashape software. Species annotations were done by observers in the field.
Data analysis	All analyses and figures were generated using the statistical software R, described in the methods, and available on GitHub.

For manuscripts utilizing custom algorithms or software that are central to the research but not yet described in published literature, software must be made available to editors/reviewers. We strongly encourage code deposition in a community repository (e.g. GitHub). See the Nature Research guidelines for submitting code & software for further information.

Data

Policy information about availability of data

All manuscripts must include a data availability statement. This statement should provide the following information, where applicable:

- Accession codes, unique identifiers, or web links for publicly available datasets
- A list of figures that have associated raw data
- A description of any restrictions on data availability

Source data and code for analysis and figures are available at the public GitHub repository, https://github.com/jmadin/surface_geometry

Field-specific reporting

Please select the one below that is the best fit for your research. If you are not sure, read the appropriate sections before making your selection.

☐ Life sciences ☐ Behavioural & social sciences ☒ Ecological, evolutionary & environmental sciences

Ecological, evolutionary & environmental sciences study design

All studies must disclose on these points even when the disclosure is negative.

Study description	The study collected structure from motion photogrammetry data from 21 sites at Lizard Island on Australia's Greta Barrier Reef, which is explained in detail in the main text and methods. Two products were generated for each site: (1) a digital elevation model, and (2) an orthomosaic. Coral colonies on the orthomosaics from the large plot at one site were annotated with coral species in the field.
Research sample	The habitat structure within 21 plots around a continental island. The habitat structure is formed by scleractinian corals. A large plot at one site additionally captured approximately 10,000 coral colonies of 150 species of coral to access biodiversity patterns in relation to habitat structure.
Sampling strategy	The 21 sites were chosen to reflect the same light environment (reef flat) at the full spectrum of reef habitats encircling the continental island. We targeted 10,000 coral colony identifications in the large plot in order to capture biodiversity variation in the 250 four square meter sub-samples.
Data collection	All authors helped collect the data as per the study description above.
Timing and spatial scale	The study was conducted over several years 2014-2015. The spatial scale of the study was the whole of Lizard Island, a continental island surrounded by coral reef.
Data exclusions	None.
Reproducibility	All data and code are provided to reproduce our work outlined in the paper.
Randomization	Study sites were selected haphazardly encircling Lizard Island. All site were shallow reef crest habitat to control for light and other environmental factors.
Blinding	All species annotations were checked independently by two or more observers to ensure consistency.

Did the study involve field work? ☒ Yes ☐ No

Field work, collection and transport

Field conditions	There were three field campaigns over two years, each for multiple weeks. Conditions were average and would not influence the quality of the data presented.
Location	Lizard Island, Great Barrier Reef, Australia.
Access and import/export	Study sites were selected haphazardly encircling Lizard Island. All site were shallow reef crest habitat to control for light and other environmental factors.
Disturbance	The study was observational only.

Reporting for specific materials, systems and methods

We require information from authors about some types of materials, experimental systems and methods used in many studies. Here, indicate whether each material, system or method listed is relevant to your study. If you are not sure if a list item applies to your research, read the appropriate section before selecting a response.

Materials & experimental systems

n/a	Involved in the study
☒	☐ Antibodies
☒	☐ Eukaryotic cell lines
☒	☐ Palaeontology
☐	☒ Animals and other organisms
☒	☐ Human research participants
☒	☐ Clinical data

Methods

n/a	Involved in the study
☒	☐ ChIP-seq
☒	☐ Flow cytometry
☒	☐ MRI-based neuroimaging

Animals and other organisms

Policy information about studies involving animals; ARRIVE guidelines recommended for reporting animal research

Laboratory animals	*For laboratory animals, report species, strain, sex and age OR state that the study did not involve laboratory animals.*
Wild animals	Scleractinian reef corals.
Field-collected samples	*For laboratory work with field-collected samples, describe all relevant parameters such as housing, maintenance, temperature, photoperiod and end-of-experiment protocol OR state that the study did not involve samples collected from the field.*
Ethics oversight	None required.

Note that full information on the approval of the study protocol must also be provided in the manuscript.